Appl Phys B (2012) 106:1019–1025
DOI 10.1007/s00340-011-4789-4

Applied Physics B
Lasers and Optics

UV-violet emission properties of $^2F(2)_{5/2}$ energy level of Nd^{3+} ions in ZBLAN glass

M. Klimczak · R. Piramidowicz

Received: 27 June 2011 / Revised version: 28 August 2011 / Published online: 11 November 2011

Abstract In this work the short-wavelength emission properties are investigated for the highest observed 4f metastable energy level $^2F(2)_{5/2}$ of Nd^{3+} ions in fluorozirconate ZBLAN glass. Various dopant concentrations, ambient temperatures and excitation conditions have been considered throughout the study. Distinct spectral features were observed under pulsed and cw excitation at 514 nm. In particular, pulsed pumping enabled recording of $^2F(2)_{5/2}$ emission spectra, not observable under CW excitation, as well as the level's fluorescence decay dynamics and its evolution with temperature and dopant concentration. According to the best of the authors' knowledge, neither the fluorescence lifetime of $^2F(2)_{5/2}$ of Nd^{3+} in ZBLAN, nor its concentration dependent evolution were reported before.

1 Introduction

Various key modern technologies depend on sources of short-wavelength, coherent radiation, particularly in the UV-violet spectral range. Present research effort in this area is focused mainly on wide band-gap semiconductors based on GaN, being intensively developed since the second half of the 1990s. This has already resulted in an impressive outcome—a wide selection of so-called "blue lasers" is commercially available at relatively low cost, offering output powers up to 1 W. Nevertheless, a number of advantages speak also for investigating rare-earth doped glasses. Such materials, specifically in fiber geometry, can benefit from a large number of potentially available emission wavelengths, high gain, excellent optical quality of output beam and natural tendency to single spatial mode operation, the previous two both characteristic for fiber lasers. The increasing availability of semiconductor light sources is considered as an additional advantage, enabling effective pumping by low-cost laser diodes via up-conversion processes. As for now, the most spectacular result is an up-conversion thulium-doped fiber laser operating in the UV reported by El Agmy in [1], however, it should be noted that the first UV lasing in a fiber has been obtained in neodymium-doped medium [2]. Nd^{3+} ion is best known for its excellent laser properties in the infrared and therefore is widely used in solid-state lasers, e.g. Nd:YAG systems, considered as a working horse in many labs and enterprises [3]. It should be noted, however, that neodymium possesses also interesting emission and lasing properties in the UV spectral range, associated with the $^4D_{3/2}$ and $^2P_{3/2}$ energy levels. Up-converted UV lasing originating from these bands was for the first time reported in 1988 in fluoride crystals (at 380 nm in Nd:LaF_3 and at 413 nm in $LiYF_4$) at cryogenic temperatures [4, 5]. Also the photon-avalanche process in Nd:$LiYF_4$ has been reported resulting in violet lasing at 413 nm under 603 nm pumping [6]. In general, short-wavelength emission and laser action in Nd^{3+} ions has been almost exclusively limited to low-phonon materials, based primarily on fluoride crystals and glasses, and to up-converted pumping, which seems to be slightly surprising, but has a relatively simple and convincing explanation [7]. Among the low-phonon materials ZBLAN glass benefits from at least two advantages in the context of UV-violet up-conversion lasing: it alone

M. Klimczak (✉)
Institute of High Pressure Physics UNIPRESS, Polish Academy of Sciences, Sokołowska 29/37, 01-142 Warsaw, Poland
e-mail: mklimcz@unipress.waw.pl
Fax: +48-22-8760452

R. Piramidowicz
Institute of Microelectronics and Optoelectronics, Warsaw University of Technology, Koszykowa 75, 00-662 Warsaw, Poland

maintains reasonable transmission in this spectral range and may be drawn in form of optical fibers, which in a natural way support the up-conversion processes by high intensities and excellent overlapping of the signals propagating in the single mode core. Room-temperature lasing at 381 and 412 nm corresponding to the $^4D_{3/2}$–$^4I_{11/2}$ and $^2P_{3/2}$–$^4I_{11/2}$ transitions was obtained for the first time in 1994 in a Nd^{3+}:ZBLAN optical fiber excited with a single wavelength of 590 nm from a dye laser [2]. It has been confirmed that infrared pumping at ca. 796 nm also results in UV-violet emissions from both $^4D_{3/2}$ and $^2P_{3/2}$ levels of neodymium due to an energy transfer processes. It is not efficient enough for stimulated emission though [8, 9]. Analysis of Nd^{3+} energy levels' locations allows pointing out of a possibility to obtain laser action on transition from the $^2P_{3/2}$ level under excitation with two wavelengths available from semiconductor sources (805 nm and 680 nm). Despite the occurrence of this pumping scheme in literature [10], there have been no further investigations in this area. Apart from the above discussed emission pathways, Nd-doped optical materials enable also short-wavelength emission from the high-lying $^2F(2)_{5/2}$ level, which have been reported in fluoride crystals under high-energy single-photon excitation [11, 12], and in oxide glasses [13, 14] pumped with 532 nm. Finally, Funk and Eden observed various UV and visible transitions attributable to $^2F(2)_{5/2}$ energy level (along with emissions related to $^4D_{3/2}$ and $^2P_{3/2}$ levels) in Nd:ZBLAN fibers pumped with a combination of CW red and infrared wavelengths (680, 740 and 800 nm) [10]. More detailed information on spectroscopic properties of neodymium's $^2F(2)_{5/2}$ emissions are sparse, which is partly related with the small ground-state absorption cross-section at UV wavelengths (3×10^{-22} cm^2 at 259 nm in ZBLAN, [15]). This makes its single-photon excitation difficult, especially that of the $^2F(2)_{5/2}$ is located typically near the UV cut-off spectral range. Instead of this, a multi-photon pumping scheme of this level with longer-wavelength photons could be considered. In case of $^2F(2)_{5/2}$ excitation in Nd:ZBLAN, theoretically, consecutive absorption of two 514 nm photons ($^4I_{9/2} \rightarrow {}^4G_{7/2}$ ground-state absorption followed by $^4G_{7/2} \rightarrow {}^2F(2)_{5/2}$ ESA) should be an attractive solution. Although the continuous-wave 514 nm excitation in Nd:ZBLAN is known to have produced UV-violet transitions from lower $^4D_{3/2}$ and $^2P_{3/2}$ levels [16], there have been no reports on short-wavelength properties of Nd:ZBLAN under pulsed 514 nm pumping. In this work we report the results of our recent studies on optical behavior of $^2F(2)_{5/2}$-originated luminescence, comparing the CW and pulsed pumping at 514 nm. Specifically, the observed UV-violet and visible emission lines have been assigned to optical transitions between this high-lying metastable level and various lower energy levels from $^4G_{11/2}$–$^2K_{13/2}$ down to $^4I_{13/2}$. The recorded $^2F(2)_{5/2}$ emission dynamics enabled identification of the level's fluorescence decay time constant, as well as its dopant concentration dependence. Differences between continuous-wave (CW) and pulsed 514 nm pumping have been explained, allowing further investigation of possible cross-relaxation channels responsible for quenching of $^2F(2)_{5/2}$ population into lower emitting levels $^4D_{3/2}$ and $^2P_{3/2}$ at higher concentrations.

2 The samples

Nd:ZBLAN bulk glass samples used in this study were fabricated at Institute of Electronic Materials Technology (ITME) Warsaw, Poland. The set comprised four bulk specimens with active ion concentrations of 0.3% mol, 1% mol, 2% mol and 5% mol. Experiments performed on this material included excitation of emission with either continuous-wave or pulsed 514 nm radiation, as well as fluorescence dynamics analysis at $T = 300$ K and $T = 10$ K.

3 Experimental

Emission spectra and fluorescence dynamic profiles were measured in a set-up comprising a Surelite OPO pumped by third harmonics of Continuum Q-switched Nd:YAG laser, CVI DK480 grating monochromator, WCT 50 Thorn-Emi PMT and Stanford Research Systems signal processing equipment controlled by a PC computer. 10 K measurements were performed with bulk samples in a closed-cycle liquid helium cryostat inserted in the optical set-up.

4 Results and discussion

Nd:ZBLAN emission spectra recorded at room temperature for a diluted sample (0.3% mol) under 514 nm CW and pulsed excitation are shown in Fig. 1 (spectra recorded for the diluted sample at $T = 10$ K were nearly identical, and therefore are not presented in this work). The spectrum obtained under CW excitation consists of four main emission lines and exhibits the same spectral features as Nd:ZBLAN emission characteristics observed under pulsed excitations at 355 nm, 585 nm and 796 nm discussed in detail in [9, 15]. The spectrum recorded under pulsed excitation at 514 nm (see Fig. 1b) differs significantly from these all. It also consists of four main emission lines in the UV, violet and blue range, but in this case they are centered at 386 nm, 420 nm, 440 nm, and 470 nm, respectively. What is more, in the near-UV two additional weak emission lines can be noticed located at around 287 nm and 305 nm as well as two broad emission bands in the green and red spectral range. These

specific spectral features result most probably from transitions from the high-lying $^2F(2)_{5/2}$ level of neodymium, located at 38595 cm^{-1} [17] and are not observable under CW excitation, being privileged only by pulsed pumping.

Assuming that $^2F(2)_{5/2}$ is the upper level of the observed transitions, the maxima should match barycenters of the expected terminating levels for individual transitions. Figure 2 shows this emission spectrum scaled in wavenumbers with respective part of Nd^{3+} energy structure in the background. The strongest emission line, centered at 386 nm, matches well the $^2H_{9/2}$–$^4F_{5/2}$ levels as its terminating band, while all the remaining emission lines match the nearby states, indicating $^2F(2)_{5/2}$ as their probable origin. Signals at wavelengths of 300 nm and shorter were faint, but evidently attributable to transitions terminating at $^4I_{15/2}$ and $^4I_{13/2}$, and on the contrary to what could be desired, no traces of $^2F(2)_{5/2}$–$^4I_{11/2,9/2}$ emissions were observed.

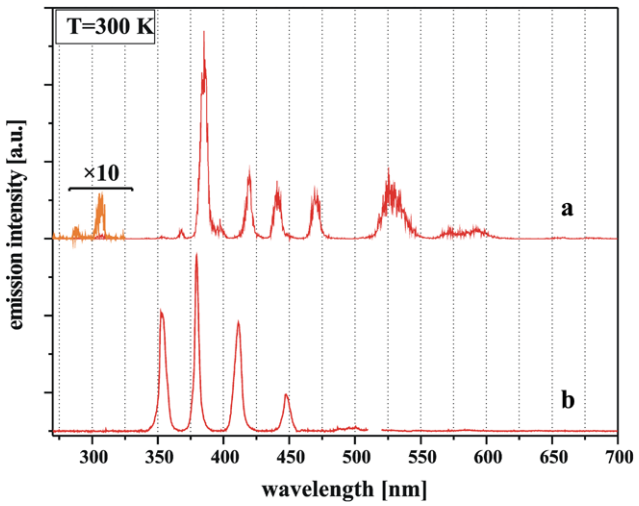

Fig. 1 Nd:ZBLAN (0.3% mol) up-conversion emission spectrum recorded at $T = 300$ K under 514 nm pumping (**a**) pulsed and (**b**) CW

All the major short-wavelength transitions observable on 514 nm pulsed-excited emission spectrum (289 nm, 305 nm, 419 nm, 441 nm, 470 nm) yield the same dynamics profiles, further supporting their association to a single emitting level. Figure 3 shows fluorescence dynamics profiles recorded for the lowest dopant concentration Nd:ZBLAN sample at room and cryogenic temperatures ($T = 300$ K and $T = 10$ K, respectively) and monitored at the strongest UV line centered at 386 nm ($^2F(2)_{5/2} \rightarrow {}^2H_{9/2} + {}^4F_{5/2}$).

Recorded fluorescence decay profiles of $^2F(2)_{5/2}$ emissions for the diluted sample (0.3% mol.) are almost purely exponential and yield time constants of 11.4 µs (±0.23 µs) at $T = 300$ K and 10.4 µs (±0.24 µs) at $T = 10$ K. It should be noted that this behavior differs from the typically observed increase of fluorescence decay time with decreasing temperature. A comparison of these values with known fluorescence lifetimes of this energy level in other optical materials is given in Table 1.

Measured evolution of $^2F(2)_{5/2}$ fluorescence decay time (defined by a drop in observed emission intensity by a factor of e^{-1}) with Nd^{3+} concentration in ZBLAN at $T = 300$ K and $T = 10$ K is given in Fig. 4. Comparison of fluorescence decay times, as well as their dopant concentration dependence, points out that room-temperature conditions slightly extend the observed decay time constants, instead of shortening it, versus cryogenic temperatures, as could be expected. This phenomenon probably stems from cross-relaxation channels most effectively affecting the lowest

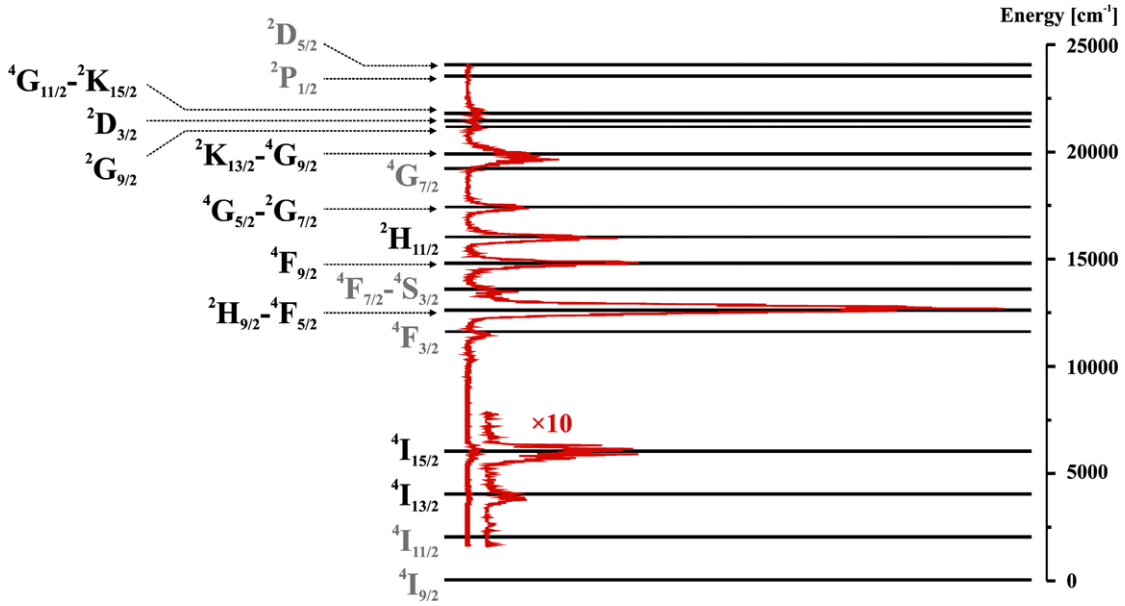

Fig. 2 Nd:ZBLAN energy level scheme and emission spectrum observed under 514 nm pulsed excitation

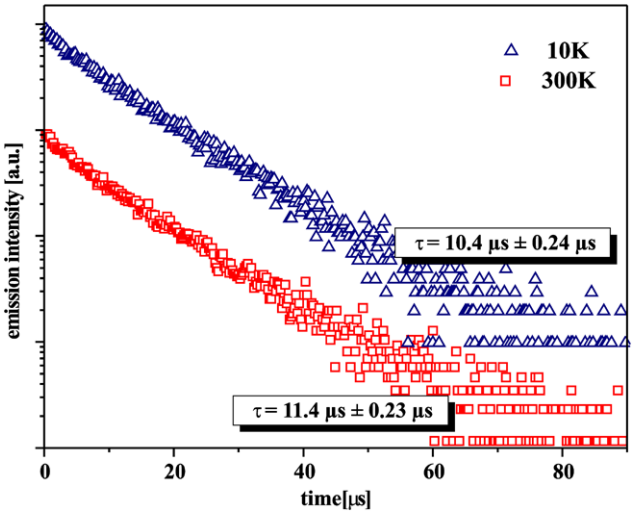

Fig. 3 Fluorescence decay profiles of $^2F(2)_{5/2}$ levels of Nd:ZBLAN (0.3% mol) recorded under 514 nm pulsed excitation at $T = 300$ K and $T = 10$ K, emission monitored at 386 nm

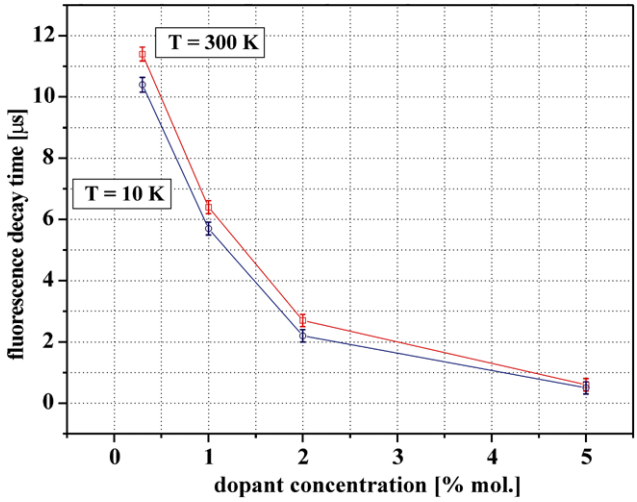

Fig. 4 Evolution of $^2F(2)_{5/2}$ fluorescence decay times with Nd^{3+} concentration at $T = 300$ K and $T = 10$ K. Pulsed excitation at 514 nm, emission monitored at 386 nm. *Solid lines* are only guides for an eye

Table 1 Fluorescence lifetime of $^2F(2)_{5/2}$ energy level of Nd^{3+} ions in different optical materials. Data for diluted samples (Nd^{3+} concentration at 0.3% mol. or less), unless noted

Material	Fluorescence lifetime		Reference
	10 K	300 K	
ZBLAN glass	10 μs	11 μs	This work
LaF_3	23 μs	23 μs	[11]
$LiYF_4$	14 μs	8 μs[a]	[18]
BaY_2F_8	14 μs	13 μs	[18]
$NaYF_4$	7 μs	6 μs	[19]
silica glass	N.A.	1 μs	[13]
YAP	N.A.	3 μs	[14]
YAG	N.A.	5 μs	[14]

[a] 1.3% mol. sample, taken after [20]

Stark component of $^2F(2)_{5/2}$. It has to be noted that observed changes of fluorescence decay times with temperature are small, which is in general qualitative agreement with results known from other neodymium-doped optical materials (see Table 1 and references therein).

Figure 5 shows two discussed cases of excitation at 514 nm. The $^4G_{7/2}$ intermediate level, excited by GSA of 514 nm photons, at room temperature is depopulated predominantly by phonon transitions. A total rate quantifying these processes may be evaluated with the energy gap law [21] at a value of around 10^8 s^{-1}. In just over 10 ns the population at $^4G_{7/2}$ relaxes non-radiatively to lower energy levels, among which only metastable $^4F_{3/2}$ has effective energy storage capability (fluorescence lifetime: 480 μs [22]). Under continuous-wave 514 nm pumping, excited population therefore stabilizes at $^4F_{3/2}$ practically instantly. Therefore pump photons are absorbed with the greatest probability by ions either in the ground or in the $^4F_{3/2}$ state (calculation of ESA cross-section for $^4F_{3/2} \rightarrow {}^4D_{7/2}$ transition yields 2.0×10^{-21} cm^2). A stepwise absorption process of 514 nm radiation comprising $^4I_{9/2} \rightarrow {}^4G_{7/2}$ and $^4F_{3/2} \rightarrow {}^4D_{7/2}$ transitions may reach only the $^4D_{3/2}$ and $^2P_{3/2}$ emitting levels, both located well below $^4D_{7/2}$. On the contrary, if significant pump radiation is delivered within the duration of a 10 ns pump pulse (following which all excited population should return to the ground state via different radiative and non-radiative processes), arriving pump photons may interact with Nd^{3+} ions either in the ground state, or the excited $^4G_{7/2}$ state and consequently may participate in the $^4G_{7/2} \rightarrow {}^2F(2)_{5/2}$ transition. Should any multi-ion energy exchange processes be neglected (which is evident for low dopant concentration sample), 10 ns pump pulses with a 10 Hz repetition rate are not enough to effectively build up the population of the $^4F_{3/2}$ state, which could give rise to $^4F_{3/2} \rightarrow {}^4D_{7/2}$ ESA transitions finally populating $^4D_{3/2}$ and $^2P_{3/2}$ levels.

It should be noted, however, that while majority of 514 nm pulsed-excited emission lines (Figs. 1, 2) can be undoubtedly assigned to $^2F(2)_{5/2}$ level, there are still traces of emission originating from $^4D_{3/2}$ and $^2P_{3/2}$ levels, observable especially for 2% mol. and 5% mol. dopant concentrations, but detectable also in the case of diluted (0.3% mol) sample. This contribution, becoming spectrally distinguishable for the more densely doped samples, specifically at 10 K, is clearly seen in Fig. 6, comparing the spectra obtained at low temperature under 514 nm pulsed excitation for different dopant concentrations.

The contribution of transitions from the $^4D_{3/2}$ and $^2P_{3/2}$ levels is further confirmed by the shape of fluorescence dynamics profiles, shown for the diluted sample in Fig. 7,

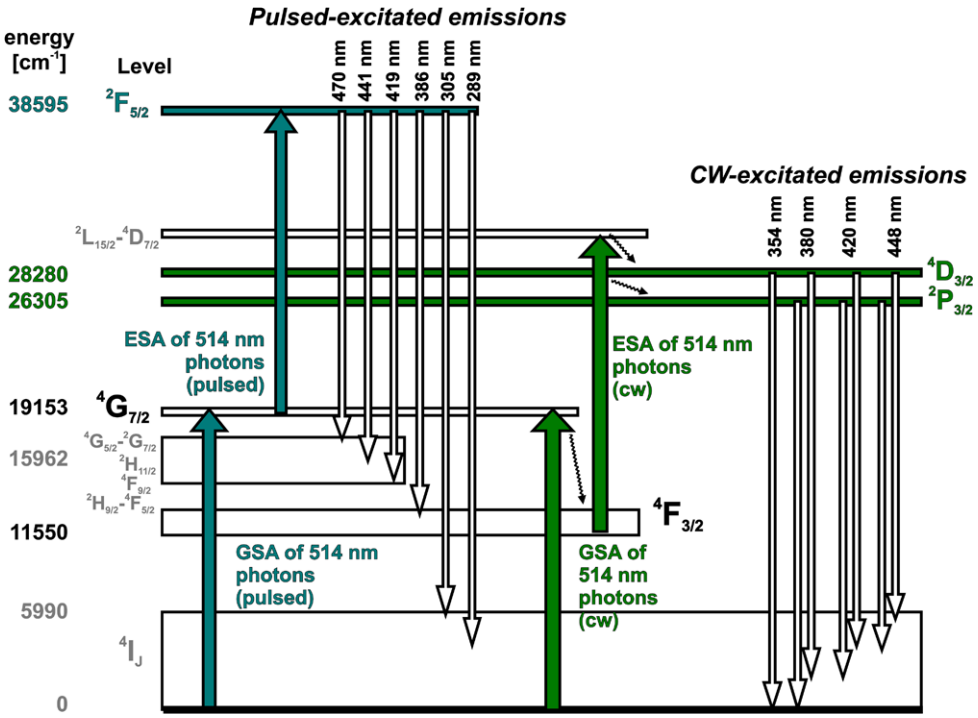

Fig. 5 Schematic excitation schemes, intermediate and anti-stokes emitting energy levels of Nd:ZBLAN under 514 nm pulsed and continuous pumping

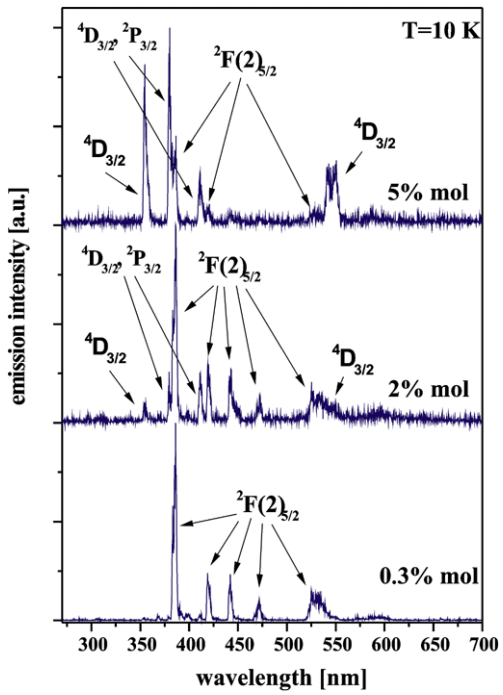

Fig. 6 Nd:ZBLAN emission spectra under 514 nm pulsed excitation for different dopant concentrations recorded at $T = 10$ K. Emission spectrum of 1% mol. did not differ significantly in these conditions and has been omitted

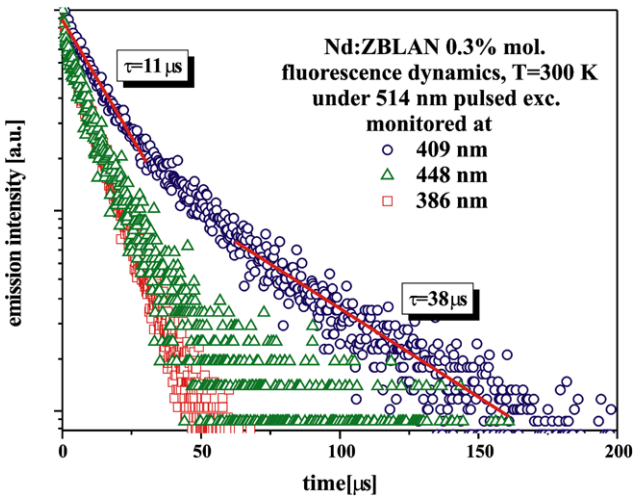

Fig. 7 Fluorescence dynamics profiles of specific spectral lines in Nd:ZBLAN (0.3% mol.) emission spectrum obtained under 514 nm pulsed excitation at $T = 300$ K

where 386 nm ($^2F(2)_{5/2} \rightarrow {}^2H_{9/2} + {}^4F_{5/2}$) dynamics is compared with 448 nm ($^2P_{3/2} \rightarrow {}^4I_{13/2}$) and 409 nm sideband (since 420 nm is completely masked with $^2F(2)_{5/2}$ emission).

The contribution of a longer component into observed emission decay profiles is evident, and its time constant of around 38 μs, characteristic for $^2P_{3/2}$, supports the thesis of its origin: $^2F(2)_{5/2}$ level is depopulated by cross-relaxation mechanisms which simultaneously populate the pair of $^2P_{3/2}$ and long-lived $^4F_{3/2}$ levels. An alternative cross-relaxation scheme is also possible, where $^2F(2)_{5/2}$ population is quenched to a group of levels between 22500 cm^{-1} and 17500 cm^{-1} (mostly ^4G_J and ^2G_J), and at the same time ground-state Nd^{3+} ions are promoted to this group,

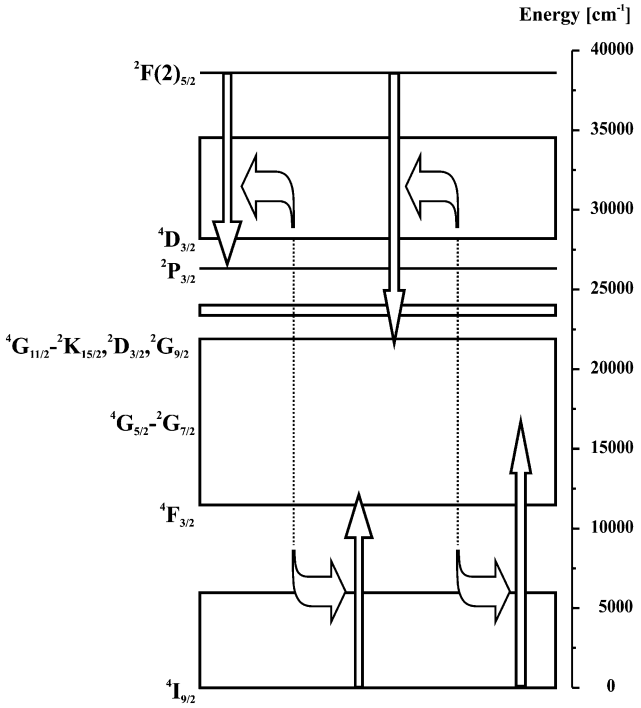

Fig. 8 $^2F(2)_{5/2}$ cross-relaxation channels resulting in population of $^2P_{3/2}$ and $^4F_{3/2}$. An alternative relaxation scheme is also shown involving ^4G_J, ^2G_J group of levels, ultimately ending up at long-lived $^4F_{3/2}$

Table 2 Total cross-relaxation rates for $^2F(2)_{5/2}$ energy level at different Nd^{3+} concentrations in ZBLAN

Nd^{3+} concentration	$^2F(2)_{5/2}$ total cross-relaxation rate (W_{CR})
1% mol	6.9×10^4 s^{-1}
2% mol	2.8×10^5 s^{-1}
3% mol	1.6×10^6 s^{-1}

as well. Since there are no Nd^{3+} metastable energy levels in this area, the population ultimately ends up relaxing down to the long-lived $^4F_{3/2}$. These two groups of cross-relaxation processes are generally depicted in Fig. 8.

The respective cross-relaxation values, calculated accordingly to the formula $I = I_0 \cdot \exp[-(W_{CR} + 1/\tau_0) \cdot \tau]$, taking the time constant of the diluted sample as τ_0, are presented in Table 2.

5 Conclusions

Spectroscopic characterization of the highest observable metastable state of Nd^{3+} ions has been performed for ZBLAN glasses. The $^2F(2)_{5/2}$ energy level experiences practically no phonon depopulation and its branching of emission lines strongly favors the 386 nm radiative transition terminating at a rapidly depopulated $^2H_{9/2} + {}^4F_{5/2}$ band. The 11 μs fluorescence decay time of $^2F(2)_{5/2}$ of Nd^{3+} ions in ZBLAN, although relatively short, is one of the longest among dielectrics matrices, where this level's emissions are observable. At higher dopant concentrations, population of this level is quenched non-radiatively to the lower lying emitting levels $^4D_{3/2}$ and $^2P_{3/2}$. Laser potential of $^2F(2)_{5/2}$ could be explored in Nd:ZBLAN optical fibers for either pulsed or continuous-wave excitation conditions. Nevertheless, pumping with short laser pulses seems impractical, as it exposes the fiber to large peak energy intensities. On the other hand, extending the duration of the 514 nm pump pulse switches excitation scheme from feeding of $^2F(2)_{5/2}$ (via $^4G_{7/2}$ level) to building up population of $^4D_{3/2}$ and $^2P_{3/2}$ (through $^4F_{3/2}$). The reason for this is a considerable, 10^8 s^{-1}, multi-phonon de-excitation rate of $^4G_{7/2}$ level down to $^4F_{3/2}$ (as shown in Fig. 5). Continuous-wave up-conversion pumping of $^2F(2)_{5/2}$ could potentially enable laser operation, but it would have to allow to pass over $^4D_{3/2}$ and $^2P_{3/2}$ in the second, excited state absorption excitation step. Such a scheme could possibly involve 808 nm laser diode excitation into $^4F_{3/2}$ level, followed by short-wavelength pumping with a GaN-based laser diode. However, reaching $^2F(2)_{5/2}$ level from $^4F_{3/2}$ (both levels are separated by no less 26000 cm^{-1} in ZBLAN) would still require a pump at a wavelength of around 385 nm, which fortunately does not match any strong ground-state absorption transitions in Nd:ZBLAN.

Acknowledgements The authors would like to express their gratitude to Dawid Piatkowski (Nicolaus Copernicus University, Poland) for calculating excited state absorption cross-sections for optical transitions populating the $^2F(2)_{5/2}$ energy level of Nd:ZBLAN.

References

1. R.M. El-Agmy, Laser Phys. **18**, 1 (2008)
2. D.S. Funk, J.W. Carlson, J.G. Eden, Electron. Lett. **30**, 1859 (1994)
3. W. Koechner, *Solid State Laser Engineering* (Springer, Berlin, 2006)
4. R.M.F. McFarlane, F. Tong, A.J. Silversmith, W. Lenth, Appl. Phys. Lett. **52**, 1300 (1988)
5. F. Tong, R.M. Macfarlane, W. Lenth, in *Conference on Quantum Electronics and Laser Science*. OSA Technical Digest Series, vol. 12 (1998), paper THKK4
6. W. Lenth, R.M. Macfarlane, J. Lumin. **45**, 346 (1990)
7. R. Piramidowicz, M. Klimczak, M. Malinowski, Proc. SPIE **5958**, 1 (2005)
8. A.T. Stanley, E.A. Harris, T.M. Searle, J.M. Parker, J. Non-Cryst. Solids **161**, 235 (1993)
9. M. Klimczak, M. Malinowski, R. Piramidowicz, Opt. Mater. **31**, 1811 (2009)

10. D.S. Funk, J.G. Eden, in *Rare-Earth-Doped Fiber Lasers and Amplifiers*, 2nd edn., ed. by M.J.F. Digonnet (Marcel Dekker, New York, 2001), pp. 171. Revised and Expanded
11. B. Jacquier, M. Malinowski, M.F. Joubert, R.H. Macfarlane, J. Lumin. **45**, 357 (1990)
12. B.M. van der Ende, R.L. Brooks, H.F. Tiedje, H. Sun, H.K. Haugen, J. Lumin. **117**, 13 (2006)
13. G.J. Quarles, G.E. Venikouas, R.C. Powell, Phys. Rev. B **31**, 6935 (1985)
14. M.F. Joubert, J.C. Couderc, B. Jacquier, J. Phys. IV **C7**, 385 (1991)
15. R. Piramidowicz, P. Witoński, M. Klimczak, M. Malinowski, Opt. Mater. **28**, 152 (2006)
16. F. Gan, J. Wang, Y. Chen, J. Non-Cryst. Solids **213&214**, 261 (1997)
17. M. Klimczak, M. Malinowski, R. Piramidowicz, in *Conference on Lasers and Electro-Optics (CLEO Europe)*, 14–19 June 2009, Munich, Germany (2009)
18. M.F. Joubert, B. Jacquier, C. Linares, J. Lumin. **47**, 269 (1991)
19. M.F. Joubert, B. Jacquier, C. Linares, R.M. Macfarlane, J. Lumin. **53**, 477 (1992)
20. A.F.H. Librantz, L. Gomes, S.L. Baldochi, I.M. Ranieri, G.E. Brito, J. Lumin. **121**, 137 (2006)
21. L.A. Riseberg, H.W. Moss, Phys. Rev. **174**, 429 (1968)
22. S.E. Stokowski, R.A. Saroyan, M.J. Weber, Nd-doped laser glass spectroscopic and physical properties. Lawrence National Laboratory, M-095 (1981)